



Universiteit  
Leiden  
The Netherlands

## **CP-MAS <sup>13</sup>C-NMR dipolar correlation spectroscopy of <sup>13</sup>C-enriched chlorosomes and isolated bacteriochlorophyll c aggregates of chlorobium tepidium: the self-organization of pigments is the main structural feature of chlorosomes**

Balaban, T.S.; Holzwarth, A.R.; Schaffner, K.; Boender, G.-J.; Groot, H.J.M. de

### **Citation**

Balaban, T. S., Holzwarth, A. R., Schaffner, K., Boender, G. -J., & Groot, H. J. M. de. (1995). CP-MAS <sup>13</sup>C-NMR dipolar correlation spectroscopy of <sup>13</sup>C-enriched chlorosomes and isolated bacteriochlorophyll c aggregates of chlorobium tepidium: the self-organization of pigments is the main structural feature of chlorosomes. *Biochemistry*, 34(46), 15259-15266.  
doi:10.1021/bi00046a034

Version: Publisher's Version

License: [Licensed under Article 25fa Copyright Act/Law \(Amendment Taverne\)](#)

Downloaded from: <https://hdl.handle.net/1887/3466168>

**Note:** To cite this publication please use the final published version (if applicable).

# CP-MAS $^{13}\text{C}$ -NMR Dipolar Correlation Spectroscopy of $^{13}\text{C}$ -Enriched Chlorosomes and Isolated Bacteriochlorophyll *c* Aggregates of *Chlorobium tepidum*: The Self-Organization of Pigments Is the Main Structural Feature of Chlorosomes<sup>†</sup>

Teodor Silviu Balaban, Alfred R. Holzwarth,\* and Kurt Schaffner

Max-Planck-Institut für Strahlenchemie, P.O. Box 10 13 65, D-45413 Mülheim an der Ruhr, Germany

Gert-Jan Boender and Huub J. M. de Groot\*

Leiden Institute of Chemistry, Gorlaeus Laboratoria, Leiden University, P.O. Box 9502, NL-2300 RA Leiden, The Netherlands

Received June 30, 1995; Revised Manuscript Received September 18, 1995<sup>⊗</sup>

**ABSTRACT:** Magic angle spinning (MAS) NMR dipolar correlation spectroscopy was applied for the first time to a biologically intact system, the light-harvesting chlorosomes of the green photosynthetic bacterium *Chlorobium tepidum*. The MAS spectra provide evidence that the self-organization of many thousands of bacteriochlorophyll *c* (BChl *c*) molecules is the predominant structural feature of the chlorosome.  $^{13}\text{C}$ -Enriched chlorosomes were prepared from nonuniformly labeled cultures grown with  $\text{NaH}^{13}\text{CO}_3$  as the main carbon source and from a uniformly  $^{13}\text{C}$ -labeled culture grown with  $\text{NaH}^{13}\text{CO}_3$  as the sole carbon source. For the nonuniformly labeled samples, the positions of the chlorin macrocycle originating from C-4 and C-5 of 5-aminolevulinic acid contained  $>95\%$   $^{13}\text{C}$  while the remaining positions, which could have originated also from unlabeled acetate, were labeled to  $\sim 60\%$  with  $^{13}\text{C}$ . The 1-D and 2-D MAS data of the labeled chlorosomes, when compared with data on the isolated labeled BChl *c* aggregated in *n*-hexane, show that the major component of the MAS signals in the chlorosomes is from BChl *c*, and only minor signal contributions arise from lipids and proteins. The  $^{13}\text{C}$  MAS signals of the BChl *c* aggregates were fully assigned by MAS 2-D dipolar correlation spectroscopy, using data on monomeric BChl *c* in  $\text{CDCl}_3/\text{CD}_3\text{OD}$  as reference. The 2<sup>1</sup>-, 3-, 3<sup>2</sup>-, 5-, 12<sup>1</sup>-, 13-, and 13<sup>1</sup>-carbons are shifted by 2.5 ppm or more upfield with respect to the solution data. The 2-D response of the BChl *c* in intact chlorosomes is virtually indistinguishable from that of the *in vitro* aggregate with respect to chemical shifts, line widths, and relative intensities of the cross-peaks. This corroborates previous evidence that self-assembly of BChl *c*, without the interaction with protein, provides the structural basis for the BChl *c* organization *in vivo*.

Green photosynthetic bacteria, such as the recently discovered species *Chlorobium tepidum* (Wahlund *et al.*, 1991), use extramembraneous chlorosomal antenna systems to harvest sunlight. Chlorosomes are oblong bodies attached to the inner side of the cytoplasmic membrane. Tubular structures, 5–10 nm wide depending on the bacterium species, could be observed in freeze-fractured chlorosomes by electron microscopy (Staelin *et al.*, 1978, 1980) [for reviews see Blankenship *et al.* (1988) and Holzwarth *et al.* (1992)]. The molecular architecture of these antenna systems is still a matter of debate. On the one hand, until quite recently proteins have been considered essential for the mutual orientation and organization of pigment molecules in *all* antenna systems, including chlorosomes (Wechsler *et al.*, 1985; Scherz & Parson, 1986; Niedermeier *et al.*, 1992; Lehmann *et al.*, 1994). On the other hand, there has been growing evidence over the past years that in chlorosomal antennae an entirely different organizational principle is in fact realized: direct chromophore–chromophore interaction

in large aggregates without the interaction with a protein as structure-forming element (Smith *et al.*, 1983; Brune *et al.*, 1987; Holzwarth *et al.*, 1990; Griebenow *et al.*, 1990; Hildebrandt *et al.*, 1990; Matsuura & Olson, 1990).

Bystrova *et al.* (1979) were the first to show that one can reproduce well the long-wavelength absorption of native chlorosomes (740–750 nm) with *in vitro* aggregates of BChl *c*<sup>1</sup> in nonpolar solvents. Numerous spectroscopic studies have since been carried out on artificial BChl *c* and *d* aggregates in solution (Causgrove *et al.*, 1990; Olson & Pedersen, 1990; Olson & Cox, 1991; Miller *et al.*, 1993; Hildebrandt *et al.*, 1994; Tamiaki *et al.*, 1994a,b; Chiefari *et al.*, 1995). It has not been possible to crystallize either chlorosomes or BChl *c* aggregates so far. Biochemical evidence that chlorosomal structures do not require the presence of proteins was first reported by Griebenow and Holzwarth (1990). This finding was later supported by various spectroscopic studies, in particular by comparison

<sup>†</sup> This research was supported in part by the Netherlands Foundation for Life Sciences, financed by the Netherlands Organization for Scientific Research (NWO).

\* To whom correspondence should be addressed.

<sup>⊗</sup> Abstract published in *Advance ACS Abstracts*, November 1, 1995.

<sup>1</sup> Abbreviations: BChl *c*, bacteriochlorophyll *c*; CP, cross-polarization; ESI, electron spray ionization; FAB, fast atom bombardment; FT-IR, Fourier-transform infrared; HPLC, high-performance liquid chromatography; MAS, magic angle spinning; MS, mass spectrometry; NMR, nuclear magnetic resonance; PAGE, polyacrylamide gel electrophoresis; RFDR, radiofrequency-driven dipolar recoupling.

of the resonance Raman spectra of protein-containing and protein-free chlorosomes which did not show any differences in the BChl *c* organization in the complete absence of proteins (Hildebrandt *et al.*, 1990). Solid-state NMR spectroscopy is another potent technique to address the problem of chlorosome structure at the atomic level including questions concerning any BChl *c* interaction with proteins (Smith & Griffin, 1988). Early solid-state NMR spectra (Nozawa *et al.*, 1990, 1991a) of natural  $^{13}\text{C}$  abundance samples showed a low signal-to-noise ratio. A more recent study by the same authors also presents data on  $^{13}\text{C}$ -labeled BChl *c* aggregates (Nozawa *et al.*, 1994). This paper confirmed conclusions concerning the central bonding network which had been derived previously from other spectroscopic data (Hildebrandt *et al.*, 1990). However, the structural model proposed therein is not unequivocally backed by the presented NMR results.

Our present data on  $^{13}\text{C}$ -labeled chlorosomes and BChl *c* aggregates were obtained by cross-polarization magic angle spinning (CP-MAS)  $^{13}\text{C}$ -NMR dipolar correlation spectroscopy (Boender *et al.*, 1995). This method is based on the RFDR pulse sequence developed by Bennett *et al.* (1992). For the first time this powerful method has been applied here to an intact biological system. The nearly complete assignment of BChl *c*  $^{13}\text{C}$  resonances in both samples confirms our previous conclusions that self-organization of BChl *c* is the predominant structural feature encountered in the chlorosomes and that proteins are not required for the mutual orientation of the BChl *c* molecules.

## MATERIALS AND METHODS

*C. tepidum* was grown anaerobically at 47 °C in 1-L culture bottles under illumination with two 40-W fluorescent neon tubes situated 30 cm from the bottles (low-light conditions). For the nonuniformly  $^{13}\text{C}$ -labeled cultures, in the growth medium (Wahlund *et al.*, 1991) the sodium hydrogen carbonate was replaced with 99%  $\text{NaH}^{13}\text{CO}_3$  (Campro Sci., Emmerich, Germany). After approximately 2 days the growth rate decreased, presumably because of self-shading. The incorporation of the  $^{13}\text{C}$  label was nonuniform because of the presence of unlabeled ammonium acetate (1:4 by weight to  $\text{NaH}^{13}\text{CO}_3$ ) as an alternative carbon source in this culture medium. While the 5- and 10-BChl *c* ring carbons were labeled to >95%, the 3<sup>1</sup>-carbon was shown by  $^1\text{H}$ -NMR to be only ~60% labeled (supporting information). This indicates that the precursor molecule in the BChl *c* biosynthesis, 5-aminolevulinic acid, had C-4 and C-5 formed exclusively out of  $\text{NaH}^{13}\text{CO}_3$  while the other carbons arose also from unlabeled acetate. Since the biosynthesis of lipids proceeds *via* acetate, the fatty acid residues were also only partially labeled. This nonuniform labeling procedure has the advantage of selectively increasing the  $^{13}\text{C}$ -NMR signals of the BChl *c* in the chlorosomes. In the cultures with  $\text{NaH}^{13}\text{CO}_3$  as the sole carbon source (ammonium acetate depleted), the growth rate was three times slower but the incorporation of the label was uniform [better than 95% [U- $^{13}\text{C}$ ] after two batch cultures]. The isotopic incorporation was determined by fast atom bombardment (FAB) and electrospray (ESI) mass spectrometry, and by  $^1\text{H}$ -NMR integration of the low-field protons ( $\delta$  9.55, doublet,  $J = 153.3$  Hz, for 5-H;  $\delta$  9.39, doublet,  $J = 152.7$  Hz, for 10-H;  $\delta = 6.22$ , doublet,  $J = 142.5$  Hz, for 3<sup>1</sup>-H). NMR

data were obtained both from nonuniformly and from the uniformly labeled samples of chlorosomes and BChl *c* aggregates.

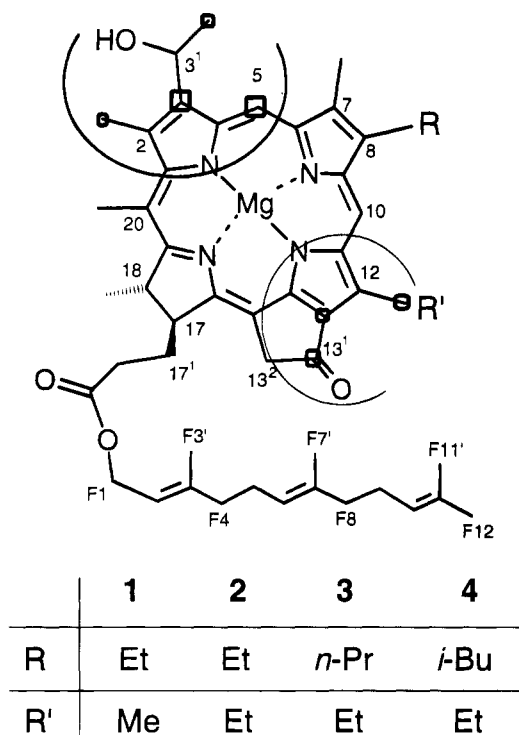
Chlorosomes were isolated as described earlier (Griebenow & Holzwarth, 1990) except that the labeled chlorosomes sedimented more rapidly during the sucrose density centrifugation due to their increased mass. A continuous sucrose concentration gradient increasing up to 40% was used. Sucrose was removed by resuspending the chlorosomes twice in tris(hydroxymethylene)aminomethane hydrochloride buffer (Tris, pH = 8.0) and recentrifugation (Beckmann ultracentrifuge, 4 °C, 45 000g, 30 min). The labeled chlorosome suspension in Tris buffer showed the expected visible absorption maximum at 748 nm and fluorescence emission bands at 777 and 804 nm (excitation wavelength being 460 nm). The chlorosome pellet was kept in the dark below 4 °C and was used to fill a 4-mm NMR rotor.

The various free BChl homologs were extracted into methanol from the labeled cells after sonication and separation of the chlorosome suspension in Tris. The filtered methanolic extract was evaporated to dryness *in vacuo* and in the dark without heating above 20 °C. BChl *c* was purified from lipids and carotenoids from the cell debris by several hexane washings and consecutive centrifugations. BChl *c* aggregates (in the natural mixture of homologs and diastereomers) were prepared by dissolving the residue in a minimal amount of dry methylene chloride followed by filtering through cotton and final precipitation upon slow addition to a large excess of *n*-hexane. The absorption maximum of the hexane layer was at 742 nm, indicating aggregate formation with optical properties similar to BChl *c* in the native chlorosomes. The precipitate was collected by centrifugation (10 000 rpm, 15 min). After final drying *in vacuo*, a fine, shining black-green aggregate powder was obtained which was used to fill the CP-MAS rotor. Alternatively, pure BChl *c* homologs were separated on a reverse-phase HPLC column (Nucleosil-7-C18, 250 mm  $\times$  20 mm i.d.) by elution with methanol:water 95:5. The main HPLC-separated fraction of (3<sup>1</sup>*R*)-[Et,Et]BChl *c*<sub>F</sub> (**2**) that was nonuniformly labeled with  $^{13}\text{C}$  was concentrated *in vacuo* to dryness. Hexane was used to wash away any traces of fatty esters from the HPLC column. Methanol traces were removed by dissolving the residue in methylene chloride and extraction with brine. After the organic solution was dried over  $\text{Na}_2\text{SO}_4$  and concentrated *in vacuo*, the residue was dissolved in a minimum amount of dry methylene chloride. This concentrated solution was filtered through cotton and was aggregated in a large excess of *n*-hexane. The precipitated aggregates were collected by centrifugation (10 000 rpm, 15 min). For the nonuniformly labeled **2**, 30 mg of aggregate was used to fill the NMR rotor, whereas the other MAS sample weights were over 80 mg.

Transesterification of the farnesyl side chain with methanol was effected by stirring under argon in the dark and at room temperature in the presence of anhydrous potassium carbonate. The yield was over 90% after purification by HPLC.

$^{13}\text{C}$  CP-MAS spectra were recorded on a Bruker MSL-400 spectrometer using a 4-mm MAS probe (Bruker, Karlsruhe, Germany). The spinning rate about the magic angle was stabilized with a home-built spinning speed controller (de Groot *et al.*, 1988). Several spinning speeds (7 000, 8 000, 10 000, and 11 000 Hz) were used in order to assign the sidebands. Absorption mode dipolar correlation

Scheme 1. BChl *c* Homologs from *C. tepidum*<sup>a</sup>



<sup>a</sup> Squares on carbon atoms indicate chemical shift differences ( $\Delta\delta$ ) between solution and solid state data. The sizes of squares are roughly proportional to the  $\Delta\delta$  values (see Table 2). Partial ellipses indicate regions of binding and overlap with other BChl *c* molecules (see text).

Table 1: Retention Times ( $t_r$ , min), Composition of the BChl *c* Mixture (%) and FAB Molecular Peaks ( $m/z$ , Da) for Components 1–5

	<b>1</b>	<b>2</b>	<b>3</b>	<b>4</b>	<b>5</b>
$t_r$	48.5	52.5	58	63.5	71
%	2	55	38	2	3
$m/z$	792	806	820	834	836

spectra were measured using procedures described in Boender *et al.* (1995). The spectra of the chlorosomes were recorded at  $\approx 5^\circ\text{C}$  in order to maintain the sample quality.

Solution spectra in  $\text{CDCl}_3$ : $\text{CD}_3\text{OD}$  (9:1 v/v) were obtained at 400 MHz for <sup>1</sup>H and at 100.61 MHz for <sup>13</sup>C on a Bruker AM 400 spectrometer for the unlabeled homologs **1–4** and for the methyl bacteriopheophorbides **Me-2** and **Me-3**. FAB and ESI MS were performed with a Finnigan MAT 95 instrument.

## RESULTS AND DISCUSSION

Scheme 1 shows the BChl *c* homologs while Table 1 summarizes the retention times and FAB molecular ions. Figure 1, trace *a*, presents the proton-decoupled <sup>13</sup>C CP-MAS spectrum of the nonuniformly labeled chlorosome preparation, and Figure 1, trace *b*, shows the corresponding spectrum of the *in vitro* BChl *c* aggregate prepared from the natural mixture of homologs and diastereomers isolated from non-uniformly labeled *C. tepidum* cells. The bacteriochlorophyll resonance patterns in these two spectra are strikingly similar, proving that the major component within the chlorosomes is self-aggregated BChl *c*. On closer inspection, one can identify in the chlorosome spectra (Figure 1, trace *a*) some contribution of glycolipids [mainly monogalactosyl diacylglyceride (MGDG), which is the major component in the lipid

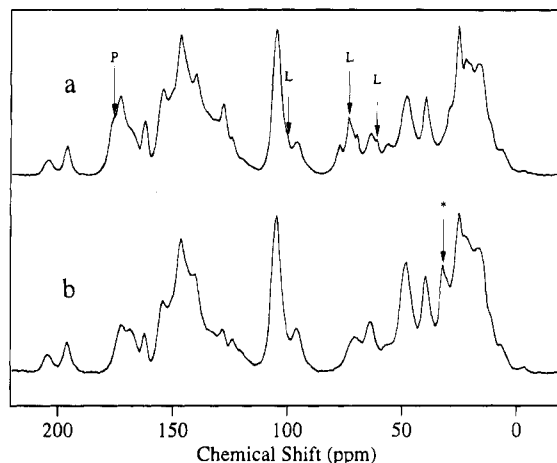


FIGURE 1: Proton-decoupled <sup>13</sup>C CP/MAS spectra of <sup>13</sup>C-labeled chlorosomes of *C. tepidum* collected at  $T \approx 278\text{ K}$  (a), and of <sup>13</sup>C-labeled *in vitro* BChl *c* aggregates collected at ambient temperature (b). Both spectra were recorded at a spinning speed of  $\omega_r/2\pi = 10\,000 \pm 5\text{ Hz}$ . Arrows indicate galactolipid peaks (L) and protein peaks (P) in the chlorosome spectra. The asterisk indicates a peak due to *n*-hexane, which was trapped by the BChl *c* aggregates and which is not removable even by placing the sample under high vacuum.

monolayer surrounding the chlorosomes (Staelin *et al.*, 1980; Holo *et al.*, 1985)] with peaks around  $\delta_C 20$  due to the apolar fatty acid residues, around  $\delta_C 60\text{--}80$  due to the sugar residue, small shoulders around  $\delta_C 100$  due to the anomeric carbon and around  $\delta_C 180$  due to the ester carbonyl groups. These are the only regions where differences between the two spectra of chlorosomes and *in vitro* BChl *c* aggregates are encountered. Of significance is also the absence in the chlorosome spectra of peaks which could be attributed to carotenoids. This is on the one hand due to the low carotenoid content in the chlorosome pellet, which was about 3% by weight as determined after chromatographic separation of an *n*-hexane extract (silica gel column eluted with *n*-hexane:diethyl ether 9:1). On the other hand, there are no signals in the <sup>13</sup>C-NMR spectrum of carotenoids that do not overlap with the signals of BChl *c*.

Previous CP-MAS spectra at natural <sup>13</sup>C abundance (Nozawa *et al.*, 1991a) allowed the assignment of only a few signals. In order to arrive at a complete assignment, we recorded two-dimensional (2-D) absorption mode dipolar correlation spectra (Boender *et al.*, 1995). Figure 2A shows such a spectrum with a relatively short evolution time (1 ms) for the chlorosome sample, while Figure 2B presents the corresponding spectrum of the *in vitro* BChl *c* aggregates under identical conditions. The observed cross-peaks in these spectra with short mixing times are predominantly associated with nearest-neighbor carbon–carbon correlations, which greatly facilitates the assignment. For instance, the carbonyl carbon 13<sup>1</sup> at  $\delta_C 196$  shows a cross-peak at  $\delta_C 128$  which must be due to C-13. The latter carbon, in turn, shows a cross-peak with C-14 ( $\delta_C 162$ ). The lines in Figure 2 indicate how the correlations of the BChl *c* ring carbons give rise to a network that leads to the assignment of the signals, similar to the procedures used in solution NMR studies. In Figure 3 the effect of increasing the mixing time (to 10.2 ms) is illustrated with correlation spectra collected at a high spinning speed,  $\omega_r/2\pi = 11\,000\text{ Hz}$ , of the nonuniformly <sup>13</sup>C-labeled chlorosome sample. The dashed-dotted lines indicate a correlation between a peak at 177 ppm and resonances

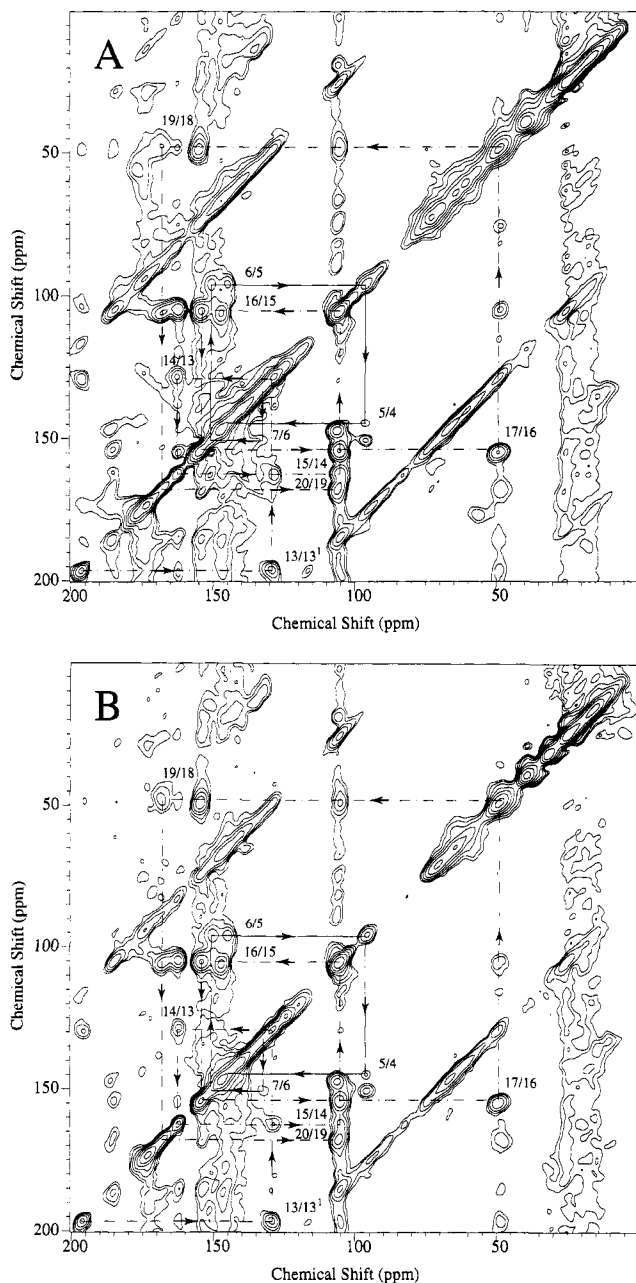


FIGURE 2: Contour plots of absorption mode MAS 2-D RFDR  $^{13}\text{C}$  dipolar correlation spectra of  $^{13}\text{C}$ -labeled chlorosomes collected at  $T \approx 278$  K (part A) and of  $^{13}\text{C}$ -labeled *in vitro* BChl *c* aggregates collected at room temperature (part B). The same spinning speed  $\omega_r/2\pi = 8\,000 \pm 3$  Hz and the same mixing time  $\tau_m = 1$  ms were used for both parts A and B. The data were recorded with 512 data points in the  $t_2$  domain, and the same amount was used for zero filling. In the  $t_1$  dimension 128 points were recorded, and a sine-square apodization, shifted by  $\pi/2$ , was used prior to Fourier transformation in this dimension. In the  $t_2$  dimension a Lorentz-Gauss transformation with a narrowing of 50 Hz and a broadening of 200 Hz (for part A) or 120 Hz (for part B) was applied prior to Fourier transformation in this dimension. The dashed-dotted and solid lines indicate two of several sequences of nearest neighbor correlations. The assignments of correlations ( $x/y$ ) on the plot correspond with the numbering of the BChl *c* carbons indicated on the formula.

around 55 ppm that cannot be attributed to BChl *c*, since they are only present in the chlorosome spectrum of Figure 2A and not in the *in vitro* aggregate (Figure 2B). These resonances and the corresponding cross-peaks can be attributed to the carbonyl and  $\alpha$  carbons of the polypeptide chain of a small protein component in the chlorosomes.

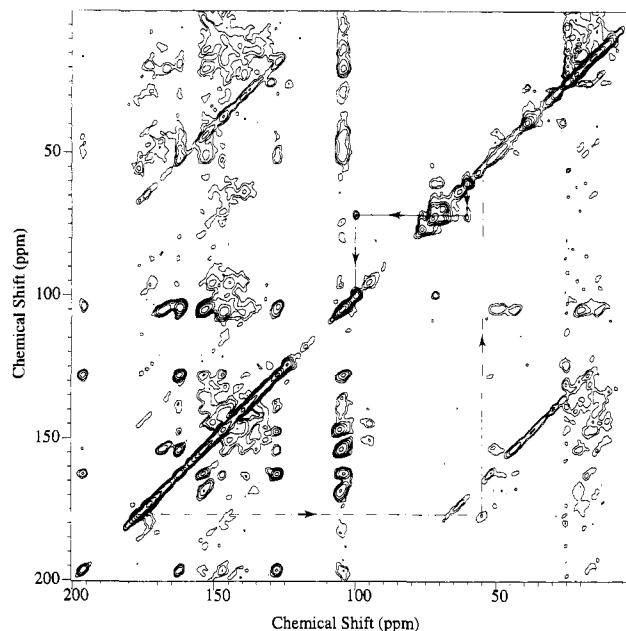


FIGURE 3: Contour plot of an absorption mode MAS 2-D RFDR  $^{13}\text{C}$  dipolar correlation spectrum of  $^{13}\text{C}$ -labeled chlorosomes collected at  $T \approx 278$  K, at a spinning speed of  $\omega_r/2\pi = 11\,000 \pm 5$  Hz and with a long mixing time  $\tau_m = 10.2$  ms. The FIDs were recorded with 512 data points, and the same amount was used for zero filling. In the  $t_1$  dimension 256 points were recorded. A sine-square apodization, shifted by  $\pi/2$ , was used in the  $t_1$  dimension prior to Fourier transformation. In the  $t_2$  dimension a Lorentz-Gauss transformation with a narrowing of 50 Hz and a broadening of 100 Hz was applied prior to Fourier transformation. The dashed-dotted lines indicate nearest neighbor correlations of the protein backbone. The solid lines indicate a cross-peak from some nearest neighbor correlations of the lipid.

When the mixing time is increased to 10.2 ms (cf. Figure 3), additional cross-peaks appear due to relayed transfer of coherence along the  $^{13}\text{C}$  backbone of the BChl *c* molecule. For instance, C-13<sup>1</sup> at  $\delta_c$  196 correlates not only with its neighbors, C-13 and C-13<sup>2</sup>, but also with the C-14 and C-15 and even weakly with C-16. In addition, new correlations appear that belong neither to BChl *c* nor to the protein, but to the galactolipids, notably at 100 ppm (X-C), 70 ppm (Y-C), and 60 ppm (2-C) as indicated by the solid lines in Figure 3. Apart from the protein and lipid contributions in the chlorosome spectrum, the cross-peaks in both spectra in Figure 2 are essentially identical with respect to chemical shifts, line widths, and intensities. This is a strong argument that the organization of the BChl *c* molecules is identical in the two systems.

The major component (2) of the BChl *c* mixture of homologs from the nonuniformly labeled culture was separated by preparative HPLC (see below and the Experimental Section) and could be aggregated in *n*-hexane similarly to the mixture. Its 1-D and 2-D CP-MAS spectra (supporting information) are almost identical to the corresponding spectra of the mixture.

The 2-D spectra were not symmetrized. A mandatory condition for intense cross-peaks is a rigid, solid sample. Carbons which have an increased mobility, such as the farnesyl and lipid carbons, do not give rise to strong cross-peaks. Essential is also the degree of the labeling in a given position. The intensity of a cross-peak decreases drastically if the labeling of one of the correlating carbons is low. If

both carbons are poorly labeled, the cross-peak may be undetectable.

An unlabeled sample of BChl *c* aggregate of the same organism and grown under similar conditions could be separated by HPLC into five components **1–5**, numbered in the increasing order of elution times (Table 1). The two major BChl *c* components (**2** and **3**), which account for over 90% of the mixture, have been identified earlier on the basis of their <sup>1</sup>H-NMR and mass spectra (Nozawa *et al.*, 1991b). We have analyzed fractions **1–4** additionally by <sup>13</sup>C-NMR in deuteriochloroform:deuteriomethanol (9:1 v/v) solution. Solution assignments are based on DEPT, H–H- and H–C-correlated spectra, NOE experiments, and gated decoupled <sup>13</sup>C-NMR spectra. Fraction **2** is a BChl *c* with ethyl groups at C-8 and C-12, and **3** has an 8-*n*-propyl group and a 12-ethyl group. While **2**, which has a (3<sup>1</sup>*R*)-hydroxy group, is diastereomerically homogeneous, **3** is a 60:40 (*R*:*S*) mixture of 3<sup>1</sup>-epimers. Fraction **1** has 8-ethyl and 12-methyl substituents. Fraction **4** is homologous to fraction **3** and has 8-isobutyl and 12-ethyl substituents. Both fractions **1** and **4** are composed of only one 3<sup>1</sup>-epimer, but, in analogy with other BChl *c* isolated from *Chlorobiaceae* (Smith & Simpson, 1986) and based on the chemical shift difference between the 5- and 10-protons, **1** has a (3<sup>1</sup>*R*) configuration and **4** a (3<sup>1</sup>*S*) configuration. All BChl *c* **1–4** are esterified with farnesol. Fraction **5** is a homogeneous 3<sup>1</sup>-epimer, esterified with a different alcohol, and with a molecular mass (FAB) of 836 Da. Its structure has not yet been determined. In conclusion, the BChl *c* samples from *C. tepidum* are characterized by a side-chain heterogeneity which cannot be neglected in solution NMR but, due to the large line widths, need not be considered in the solid-state spectra (see below).

For the purpose of comparison, the methyl bacteriopheophorbides *c*, which have the farnesyl residue shortened to a methyl group, were prepared from the main components **2** and **3** by mild transesterification with methanol in the presence of anhydrous potassium carbonate. **Me-2** and **Me-3** were thus obtained in over 90% yield after HPLC separation. This direct transesterification procedure avoids the usual two-step sequence consisting of an acid-catalyzed methanolysis followed by the reinsertion of magnesium.

Table 2 lists the solution <sup>13</sup>C chemical shifts of the individual BChl *c* components together with the solid-state chemical shifts of the chlorosomes and of the aggregates composed of the mixture of BChl *c*. The solution assignments are consistent with literature data (Smith & Goff, 1985; Fages *et al.*, 1990) with the exception that the assignment of quaternary carbons 14 and 16 had to be interchanged on the basis of the 2-D CP-MAS spectra. Considerable discrepancies exist between the recent solution assignments for the aliphatic carbons by Nozawa *et al.* (1994) and our own (see Table 2 and footnote) which take into account the C–H-correlated spectra.

When the solution chemical shifts are compared with the ones in the solid state, the largest differences ( $\Delta\delta$ ) appear for carbons 3, 5, 12<sup>1</sup>, 3<sup>2</sup>, 13<sup>1</sup>, 2<sup>1</sup>, and 13. These carbons are indicated on the formula in Scheme 1 by squares of sizes proportional to the differences  $\Delta\delta$ . Due to ring current effects from the chlorin macrocycle or due to polarization effects, shifts should be experienced by the carbons in the region of binding and overlap indicated on the formula by partial ellipses. The same regions of the molecule experience upon deaggregation with methanol the largest titration shifts

in <sup>1</sup>H-NMR solution (CDCl<sub>3</sub>) spectra (Griebenow, 1992). This represents an independent proof that the binding of BChl *c* molecules within the aggregates involves the coordination of the magnesium atom of one BChl *c* molecule to the 3<sup>1</sup>-hydroxy group of another BChl *c*. Simultaneously, hydrogen bonding to the 13<sup>1</sup>-carbonyl oxygen of a third BChl *c* molecule occurs. This is in accord with recent FT-IR and visible absorption spectra which show that in solution the bonding arrangement C=O···H–O···Mg predominates (Chiefari *et al.*, 1995). The powdery nature of our BChl *c* aggregate samples allowed us for the first time to obtain also solid-state FT-IR spectra in KBr pellets. The hydrogen bond is evident in the broad O–H deformation bands centered at about 3300–3200 cm<sup>-1</sup> and in the carbonyl stretching band at 1653 cm<sup>-1</sup>. These large shifts to much lower frequencies than normally encountered for O–H and C=O bonds, respectively, indicate an unusually strong hydrogen bond due to the increased polarization caused by the ligation to the magnesium atom (Chiefari *et al.*, 1995). The ester carbonyl group which is not involved in hydrogen bonding appears with a much lower intensity at 1730 cm<sup>-1</sup>.

Previous attempts to interpret proton shifts in solution on the basis of ring current effects have considered two dimer structures of methyl bacteriochlorophyllide *d* (Smith *et al.*, 1986), methyl pyrrochlorophyllide *a* (Abraham *et al.*, 1989), and BChl *c* (Nozawa *et al.*, 1992) as the most probable, namely, the “piggy back” and “face to face” dimers. These dimers have, however, quite a different aggregation state and different optical spectra from the “large aggregates” studied here with absorption maxima at 742 nm. An extension of the ring current calculations from proton shifts to <sup>13</sup>C-NMR shifts in the solid state was performed for BChl *c* aggregates (Nozawa *et al.*, 1994). On the basis of these calculations, various aggregation geometries were considered and rejected as unable to reproduce a 5 ppm shift for the 5-carbon which could be unequivocally assigned from the 1-D CP-MAS spectra. The only model that accounted for this large aggregation shift upon going from solution to the solid state ( $\Delta\delta$ ) was termed the “ring overlap model”. However, according to the calculations for this model (Nozawa *et al.*, 1994), several other carbon atoms, namely, 3<sup>1</sup>, 3, and 4, should have even larger  $\Delta\delta$  values, namely, 7.0, 6.8, and 5.9 ppm, respectively. On the basis of our 2-D spectra and the full assignment which has been reached, to the resonances of carbons 3<sup>1</sup> and 4 we can now ascribe  $\Delta\delta$  values of less than 1 ppm. This discrepancy sheds serious doubts both on the ring overlap model and on the assumption that  $\Delta\delta$  <sup>13</sup>C shifts arise from ring current effects alone. More probably, different polarization effects operate in the solid state due to the very special C=O···H–O···Mg bonding arrangement, and these are superimposed on the ring current effects. A similar combination of ring current shifts and polarization effects were invoked recently to explain the observed chemical shifts encountered in Chl *a*–water aggregates (Boender *et al.*, 1995). We conclude that the model for the BChl *c* organization in chlorosomes proposed by Nozawa *et al.* is inconsistent with our CP-MAS data.

The CP-MAS spectra, especially their large line widths of several hundred Hz, indicate considerable disorder of various kinds, both in the chlorosome and in the BChl *c* aggregate samples. This is in contrast to the much smaller line widths encountered in Chl *a*–water aggregates (Boender *et al.*, 1995). There is evidently no strictly unique way of

Table 2: Assignments of  $^{13}\text{C}$ -NMR Signals of BChl *c* from *C. tepidum*<sup>a</sup>

position	1	2	3	4	Me-2 <sup>b</sup>	Me-3 <sup>b</sup>	aggregate	ε	chlorosome	ε	Δδ <sup>c</sup>
13 <sup>1</sup>	198.20	197.49	197.43	197.39	197.41	197.38	195.8	(0.4)	195.8	(0.3)	2.5
17 <sup>3</sup>	173.73	173.62	173.72	173.80	174.18	174.17	172.6	(0.3)	173.0	(0.5)	1
19	167.84	167.76	167.79 <sup>d</sup>	167.94	167.79	167.80	168.5	(0.9)	168.1	(0.3)	0
14	161.08	161.24	161.33	161.31	161.35	161.35	162.1	(0.4)	162.1	(0.3)	1
16	154.27	153.98	154.14 <sup>d</sup>	154.14	154.10	154.09	154.0	(0.4)	153.6	(0.6)	0
1	153.76	153.79	153.75 <sup>d</sup>	153.77	153.78	153.75	153.9	(0.4)	153.2	(0.5)	0
6	150.69	150.72	150.60 <sup>d</sup>	150.56	150.65	150.60	150.7	(0.3)	150.6	(0.3)	0
11	147.66	146.47	146.65	147.08	146.74	146.70	146.8	(0.3)	146.8	(0.4)	0
9	146.09	146.01	146.65	146.66	146.15	146.70	146.8	(0.3)	146.8	(0.4)	0
4	145.28	145.37	145.23	145.27	145.24	145.21	144.8	(0.5)	144.7	(0.3)	0
3	145.14	145.13	145.18 <sup>d</sup>	145.11	145.17	145.11	140	(1)	139	(1)	5
8	143.48	143.39	142.46	141.12	143.58	141.85	142.4	(0.4)	142.3	(0.6)	0
F3	142.43	142.23	141.79	142.56			140.4	(0.3)	140.1	(0.3)	1.5
12	133.34	140.65	140.97	141.02	141.14	141.11	139	(1)	139	(1)	2
2	135.19	135.08	135.20	135.19	135.29	135.28	134.9	(0.3)	135.2	(0.3)	0
F7	135.14	134.98	135.20	135.27			135	(1)	135	(1)	0
7	133.63	133.45	134.28	134.78	133.70	134.35	132.5	(0.3)	132.3	(0.3)	1.5
F11	131.02	130.82	131.07	131.14			130.0	(0.3)	130.2	(0.3)	1
13	131.02	130.26	130.63	130.72	130.77	130.75	128.1	(0.3)	127.9	(0.5)	2.5
F10-CH	123.98	123.87	124.03	124.08			124	(1)	124	(1)	0
F6-CH	123.28	123.19	123.33	123.36			124	(1)	124	(1)	0
F2-CH	117.51	117.50	117.58	117.60			119.2	(0.3)	119.1	(0.3)	-1.5
10-CH	105.61	105.57	105.97	106.37	105.79	106.03	105.7	(0.3)	105.5	(0.5)	0
15	104.92	104.74	105.00	105.09	105.05	105.05	104.8	(0.3)	104.3	(0.7)	0.5
20	104.68	104.74	104.98 <sup>d</sup>	104.93	104.95	104.93	105.3	(0.3)	105.0	(0.7)	0
5-CH	100.16	100.03	100.17	100.27	100.17	100.17	95.6	(0.3)	95.5	(0.5)	4.5
3 <sup>1</sup> -CH	65.14	64.95	65.22 <sup>d</sup>	65.44	65.33	65.32	64.2	(0.3)	63.7	(0.7)	1
F1-CH <sub>2</sub>	61.30	61.14	61.34	61.42			60.7	(0.5)	60.9	(0.3)	0
17-CH	50.14	50.07	50.35 <sup>d</sup>	50.39	50.25	50.25	49.8	(0.8)	49.7	(0.4)	0
13 <sup>2</sup> -CH <sub>2</sub>	49.14 <sup>e</sup>	48.28 <sup>e</sup>	48.99 <sup>e</sup>	<i>e</i>	<i>e</i>	<i>e</i>	48.6	(0.4)	48.1	(0.4)	0
18-CH	48.19 <sup>e</sup>	47.64	48.14 <sup>e</sup>	<i>e</i>	<i>e</i>	<i>e</i>	48	(1)	48.1	(0.4)	0
F4-CH <sub>2</sub>	39.33	39.22	39.40	39.45			39.4	(0.3)	39.1	(0.3)	0
F8-CH <sub>2</sub>	39.14	39.02	39.21	39.27			39.4	(0.3)	39.1	(0.3)	0
17 <sup>2</sup> -CH <sub>2</sub>	30.70	30.60	30.83 <sup>d</sup>	30.86	30.55	30.54	30	(2)	30	(2)	0
17 <sup>1</sup> -CH <sub>2</sub>	29.69	29.60	29.76 <sup>d</sup>	29.93	29.81	29.80	30	(2)	30	(2)	0
F5-CH <sub>2</sub>	26.35	26.23	26.41	26.46			25.6	(0.4)	25.7	(0.4)	0
F9-CH <sub>2</sub>	25.83	25.70	25.89	25.95			25.6	(0.4)	25.7	(0.4)	0
3 <sup>2</sup> -CH <sub>3</sub>	25.58	25.43	25.56 <sup>d</sup>	25.74	25.67	25.64	22.5	(0.3)	22.7	(0.3)	3
F12-CH <sub>3</sub> <sup>f</sup>	25.24	25.04	25.30	25.38			25.2	(0.3)	25.2	(0.3)	0
20 <sup>1</sup> -CH <sub>3</sub> <sup>f</sup>	21.14	20.96	21.19	21.26	21.26	21.26	20	(1)	20	(1)	1
12 <sup>1</sup> -CH <sub>2</sub> <sup>f</sup>		20.77	20.96	21.03	21.04	21.04	17.5	(0.6)	17.5	(0.6)	3.5
18 <sup>1</sup> -CH <sub>3</sub> <sup>f</sup>	20.55	20.36	20.50 <sup>d</sup>	20.54	20.65	20.64	21	(1)	21	(1)	1
8 <sup>1</sup> -CH <sub>2</sub>	19.24	19.14			19.40		19	(1)	19	(1)	0
			28.08				28.14		26.0	(0.4)	2
F11'-CH <sub>3</sub> <sup>f</sup>	17.24	17.03	17.30	17.38			16.5	(0.6)	16.6	(0.6)	0.5
8 <sup>2</sup> -CH <sub>3</sub>	17.14	16.97			17.29		16.4	(0.6)	16.9	(0.6)	0.5
2 <sup>1</sup> -CH <sub>3</sub>	16.95	16.76	16.98 <sup>d</sup>	17.16	17.12	17.10	14.3	(0.7)	13.8	(0.7)	2.5
12 <sup>2</sup> -CH <sub>3</sub>		16.56	16.77	16.84	16.81	16.81	15.2	(0.6)	16.8	(0.6)	0
F3'-CH <sub>3</sub> <sup>f</sup>	15.98	15.79	16.04	16.13			16	(1)	16	(1)	0
F7'-CH <sub>3</sub> <sup>f</sup>	15.55	15.35	15.61	15.69			16	(1)	16	(1)	0
7 <sup>1</sup> -CH <sub>3</sub>	10.55	10.37	10.90	11.26	10.74	11.00	11.0	(0.3)	10.6	(0.6)	0
other signals	12.29 <sup>g</sup>		25.90 <sup>h</sup>	35.42 <sup>k</sup>	51.46 <sup>i</sup>	51.46 <sup>i</sup>					
			14.16 <sup>i</sup>	31.95 <sup>k</sup>		25.95 <sup>h</sup>					
				22.96 <sup>k</sup>		14.24 <sup>i</sup>					

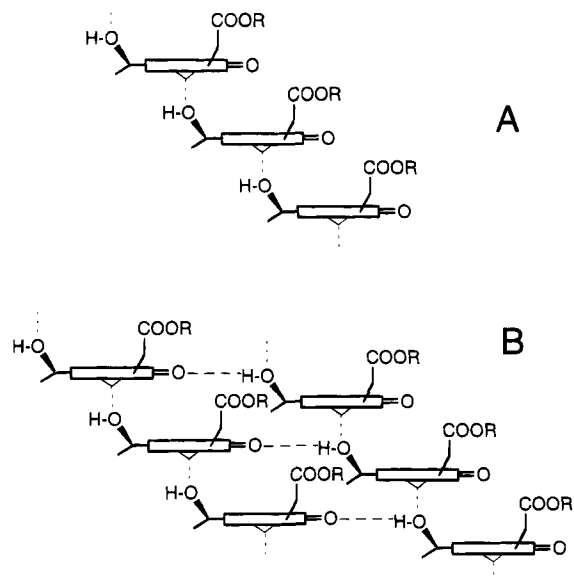
<sup>a</sup> Solution data (CDCl<sub>3</sub>:CD<sub>3</sub>OD, 9:1 v/v): chemical shifts are given in ppm relative to the CDCl<sub>3</sub> triplet set at δ 77.00. Solid-state data: chemical shifts are given in ppm relative to external glycine whose carbonyl signal was set at δ 176.04; estimated errors (ε, in ppm) are given in parentheses.

<sup>b</sup> These compounds are esterified with methanol instead of farnesol. <sup>c</sup> Average difference (in ppm) between solution and solid states. <sup>d</sup> Signal showing additional splitting due to the *R* and *S* epimers. <sup>e</sup> Visible only in DEPT spectra due to overlap with the methanol signal. <sup>f</sup> These assignments are interchanged in comparison to those of Nozawa *et al.* (1994). <sup>g</sup> 12<sup>1</sup>-CH<sub>3</sub>. <sup>h</sup> 8<sup>2</sup>-CH<sub>2</sub>. <sup>i</sup> 8<sup>3</sup>-CH<sub>3</sub>. <sup>j</sup> COOCH<sub>3</sub>. <sup>k</sup> Isobutyl carbons.

binding and orienting of the BChl *c* molecules, which should lead to a rigid structure with sharp peaks. Rather, multiple orientations or a more subtle kind of disorder must be present.

It has been shown by molecular modeling that the ligation of the magnesium atoms by the 3<sup>1</sup>-hydroxy groups can lead to the formation of stacks of the BChl *c* molecules which can form tubular structures as observed in electron microscopy (Holzwarth & Schaffner, 1994). The orientation of the molecules within a stack may not be exactly regular, so that they may be regarded as approaching a liquid crystal like state. Our model also takes into account cooperative

hydrogen bonding between stacks. The hydrogen bond acceptor is the 13<sup>1</sup>-carbonyl group while the donor is a 3<sup>1</sup>-hydroxy group which ligates a magnesium atom. In this model for the binding of BChl *c* in the chlorosomes (Holzwarth & Schaffner, 1994), tubular micelles are formed by multiple hydrogen bonds between stacks of BChl *c* molecules. A detailed analysis of intermolecular BChl *c*-BChl *c* cross-peaks in order to derive the aggregate structure from NMR data requires further work. Apart from a weak cross-peak between the 3-carbon (140 ppm) and the 13<sup>1</sup>-C=O (196 ppm), this interstack hydrogen bonding is

Scheme 2. Cartoon Models of BChl *c* Aggregates<sup>a</sup>

<sup>a</sup> The 13<sup>1</sup>-carbonyl group and the 3-hydroxyethyl group are explicit. The 17-propionyl ester groups are directed toward the observer. The magnesium atom (pictured as a triangle) may be ligated by OH groups, either from the same side as the ester group (*syn*) or, as depicted, from the opposite side (*anti*). Part A shows a trimer which can be inferred from the present NMR data. Part B shows two stacks of BChl *c* with cooperative hydrogen bonding which is inferred from FT-IR data. The C=O...H-O angle is about 150° so that each stack appears slightly rotated to the one with which it is multiply hydrogen bonded.

not strongly evident from the solid-state NMR spectra. The chemical shift differences which are encountered for the 3<sup>1</sup>-carbon and the 13<sup>1</sup>-carbonyl carbon between solution and solid state ( $\Delta\delta$ , see Table 2) could either be due to hydrogen bonding or could result from ring current shifts. However, it is possible to conclude that the overall features of our recently proposed model simulation are fully consistent with the NMR data presented here. The most important confirmation comes from the  $\Delta\delta$  values which map into two regions of binding and overlap indicated on the formula in Scheme 1 with partial ellipses. The stacks of BChl *c* which are encountered in our model (Holzwarth & Schaffner, 1994) and not in Nozawa's ring overlap model demand exactly this aggregation map, with three consecutive overlapping BChl *c* molecules. The first molecule (upper partial ellipse which is thicker and may be viewed as above the formula) has its magnesium atom ligated by the 3<sup>1</sup>-OH group of the middle BChl *c* molecule whose formula is explicit. The 13<sup>1</sup>-carbonyl oxygen of the upper molecule sits approximately above the magnesium atom of the middle BChl *c* molecule. Although this is not a proper coordination, the negative oxygen atom contributes to minimize the partial positive charge residing on the magnesium atom of the middle molecule which is ligated to the 3<sup>1</sup>-OH group of the third BChl *c* molecule sitting underneath (thinner partial ellipse). A side view of such a trimer is presented in Scheme 2, part A. It is evident that by cooperative hydrogen bonding, parallel running stacks of BChl *c* molecules can be arranged side by side (Scheme 2, part B). Molecular modeling (Holzwarth & Schaffner, 1994) shows that a curvature is formed when several stacks are joined by hydrogen bridges. This curvature is due to the interstack hydrogen bonds and does not imply a deformation of the chlorin macrocycle. Between 20 and 22 such stacks form a closed surface (a

torus) whose diameter matches not only the one encountered in the chlorosomal rods but also that encountered in the neutron diffraction studies (Worcester *et al.*, 1986) of BChl *c* and Chl *a* aggregates. Finally, from the identity of the BChl *c* signals in chlorosomes and *in vitro* BChl *c* aggregates with respect to chemical shifts, line widths, and intensities, we can conclude that proteins are not involved in the organization of the majority of Bchl *c* within the chlorosomal rods.

## CONCLUSION

We have presented evidence, based on 1-D and 2-D CP-MAS spectra of intact chlorosomes and of BChl *c* aggregates, that proteins cannot be responsible for the organization of the chlorosomal BChl *c* rods. The structure responsible for the efficient energy transfer arises thus from a supramolecular self-assembly of BChl *c* molecules. The present findings are a particularly strong support for the predominance of the pigment-pigment interaction and they complement our previous experimental data based on PAGE, linear dichroism, and resonance Raman studies. Work is currently under way to quantify the data from the 2-D CP-MAS spectra, especially at longer evolution times in the uniformly labeled chlorosomes and BChl *c* aggregates, in order to extract distance information between carbons of neighboring molecules which give dipolar correlations.

## ACKNOWLEDGMENT

We thank Prof. J. Olson for providing a starting sample of *C. tepidum* which was cultured by U. Pieper. Thanks are also due to M. Reus and K. Silbermann for help with the chlorosome isolations, to M. Trinoga for the preparative HPLC work, to J. Bitter for recording the solution NMR spectra, and to M. Massau for the MS measurements.

## SUPPORTING INFORMATION AVAILABLE

Assessment of the <sup>13</sup>C labeling by <sup>1</sup>H-NMR; <sup>13</sup>C-NMR solution spectra of **2** and of the mixture of BChl *c* homologs from the nonuniformly labeled culture; CP-MAS spectra of the **2** after HPLC at different spinning speeds; CP-MAS spectra of chlorosomes from the uniformly <sup>13</sup>C-labeled culture at different spinning speeds (nine pages). Ordering information is given on any current masthead page.

## REFERENCES

- Abraham, R. J., Rowan, A. E., Goff, D. A., Mansfield, K. E., & Smith, K. M. (1989) *J. Chem. Soc., Perkin Trans. 2*, 1633-1641.
- Bennett, A. E., Ok, J. H., Griffin, R. G., & Vega, S. (1992) *J. Chem. Phys.* 96, 8624-8627.
- Blankenship, R. E., Brune, D. C., & Wittmershaus, B. P. (1988) in *Light-Energy Transduction in Photosynthesis: Higher Plant and Bacterial Models* (Stevens, S. E., & Bryant, D. A., Eds.) pp 32-46, American Society of Plant Physiologists, Rockville, MD.
- Boender, G.-J., Raap, J., Prytulla, S., Oschkinat, H., & deGroot, H. J. M. (1995) *Chem. Phys. Lett.* 237, 502-508.
- Brune, D. C., Nozawa, T., & Blankenship, R. E. (1987) *Biochemistry*, 26, 8644-8652.
- Bystrova, M. I., Mal'gosheva, I. N., & Krasnovskii, A. A. (1979) *Mol. Biol.* 13, 582-594.
- Causgrove, T. P., Brune, D. C., Blankenship, R. E., & Olson, J. M. (1990) *Photosynth. Res.* 25, 1-10.
- Chiefari, J., Griebenow, K., Fages, F., Griebenow, N., Balaban T. S., Holzwarth, A. R., & Schaffner, K. (1995) *J. Chem. Phys.* 99, 1357-1365.

- De Groot, H. J. M., Copié, V., Smith, S. O., Allen, P. J., Winkel, C., Lugtenburg, J., Herzfeld, J., & Griffin, R. G. (1988) *J. Magn. Reson.* 77, 251–257.
- Fages, F., Griebenow, N., Griebenow, K., Holzwarth, A. R., & Schaffner, K. (1990) *J. Chem. Soc., Perkin Trans. 1*, 2791–2797.
- Griebenow, K. (1992) Ph.D. Thesis, Heinrich-Heine-Universität, Düsseldorf, Germany.
- Griebenow, K., & Holzwarth, A. R. (1990) in *Molecular Biology of Membrane-Bound Complexes in Phototropic Bacteria* (Drews, G., & Dawes, E. A., Eds.) pp 375–381, Plenum Press, New York.
- Griebenow, K., Holzwarth, A. R., & Schaffner, K. (1990) *Z. Naturforsch.* 45c, 823–828.
- Hildebrandt, P., Griebenow, K., Holzwarth, A. R., & Schaffner, K. (1990) *Z. Naturforsch.* 46c, 228–232.
- Hildebrandt, P., Tamiaki, H., Holzwarth, A. R., & Schaffner, K. (1994) *J. Phys. Chem.* 98, 2191–2197.
- Holo, H., Broch-Due, M., & Ormerod, J. G. (1985) *Arch. Microbiol.* 143, 94–99.
- Holzwarth, A. R., & Schaffner, K. (1994) *Photosynth. Res.* 41, 225–233.
- Holzwarth, A. R., Griebenow, K., & Schaffner, K. (1990) *Z. Naturforsch.* 45c, 203–206.
- Holzwarth, A. R., Griebenow, K., & Schaffner, K. (1992) *J. Photochem. Photobiol. A* 65, 61–71.
- Lehmann, R. P., Brunisholz, R. A., & Zuber, H. (1994) *FEBS Lett.* 342, 319–324.
- Matsuura, K., & Olson, J. M. (1990) *Biochim. Biophys. Acta* 1019, 233–238.
- Miller, M., Gillbro, T., & Olson, J. M. (1993) *Photochem. Photobiol.* 57, 98–102.
- Niedermeier, G., Scheer, H., & Feick, R. G. (1992) *Eur. J. Biochem.* 204, 685–692.
- Nozawa, T., Suzuki, M., Kanno, S., & Shirai, S. (1990) *Chem. Lett.* 1805–1808.
- Nozawa, T., Suzuki, M., Ohtomo, K., Morishita, Y., Konami, H., & Madigan, M. T. (1991a) *Chem. Lett.* 1641–1644.
- Nozawa, T., Ohtomo, K., Suzuki, M., Morishita, Y., & Madigan, M. T. (1991b) *Chem. Lett.* 1763–1766.
- Nozawa, T., Ohtomo, K., Morishita, Y., Konami, H., & Madigan, M. T. (1992) *Chem. Lett.* 261–264.
- Nozawa, T., Ohtomo, K., Suzuki, M., Nakagawa, H., Shikama, Y., Konami, H., & Wang, Z.-Y. (1994) *Photosynth. Res.* 41, 211–223.
- Olson, J. M., & Cox, R. P. (1991) *Photosynth. Res.* 30, 35–43.
- Olson, J. M., & Pedersen, J. P. (1990) *Photosynth. Res.* 25, 25–37.
- Scherz, A., & Parson, W. W. (1986) *Photosynth. Res.* 9, 21–32.
- Smith, K. M., & Goff, D. A. (1985) *J. Chem. Soc., Perkin Trans. 1*, 1099–1113.
- Smith, K. M., & Simpson, D. J. (1986) *J. Chem. Soc., Chem. Commun.* 1682–1684.
- Smith, K. M., Kehres, L. A., & Fajer, J. (1983) *J. Am. Chem. Soc.* 105, 8644–8652.
- Smith, K. M., Bobe, F. W., Goff, D. A., & Abraham, R. J. (1986) *J. Am. Chem. Soc.* 108, 1111–1120.
- Smith, S. O., & Griffin, R. G. (1988) *Annu. Rev. Phys. Chem.* 39, 511–535.
- Staehelein, L. A., Golecki, J. R., Fuller, R. C., & Drews, G. (1978) *Arch. Microbiol.* 119, 269–277.
- Staehelein, L. A., Golecki, J. R., & Drews, G. (1980) *Biochim. Biophys. Acta* 589, 30–45.
- Tamiaki, H., Holzwarth, A. R., & Schaffner, K. (1994a) *Photosynth. Res.* 41, 245–251.
- Tamiaki, H., Takeuchi, S., Tanikaga, R., Balaban, S. T., Holzwarth, A. R., & Schaffner, K. (1994b) *Chem. Lett.* 401–402.
- Wahlund, T. M., Woese, C. R., Castenholz, R. W., & Madigan, M. T. (1991) *Arch. Microbiol.* 156, 81–90.
- Wechsler, T., Suter, F., Fuller, R. C., & Zuber, H. (1985) *FEBS Lett.* 181, 173–178.
- Worcester, D. L., Michalski, T. J., & Katz, J. J. (1986) *Proc. Natl. Acad. Sci. U.S.A.* 83, 3791–3795.

BI951488X